NANO LETTERS

2007
Vol. 7, No. 1
45−50

DNA Nucleoside Interaction and Identification with Carbon Nanotubes

Sheng Meng,[†] Paul Maragakis,[‡] Costas Papaloukas,[§] and Efthimios Kaxiras*,[†]

Department of Physics and Division of Engineering and Applied Sciences, Harvard University, Cambridge, Massachusetts 02138, Department of Chemistry and Chemical Biology, Harvard University, Cambridge, Massachusetts 02138, and Department of Biological Applications and Technology, University of Ioannina, Ioannina 45110, Greece

Received August 14, 2006; Revised Manuscript Received November 8, 2006

ABSTRACT

We investigate the interaction of individual DNA nucleosides with a carbon nanotube (CNT) in vacuum and in the presence of external gate voltage. We propose a scheme to discriminate between nucleosides on CNTs based on measurement of electronic features through a local probe such as scanning tunneling spectroscopy. We demonstrate through quantum mechanical calculations that these measurements can achieve 100% efficiency in identifying DNA bases. Our results support the practicality of ultrafast DNA sequencing using electrical measurements.

DNA strands and carbon nanotubes (CNTs) are prototypical one-dimensional structures; the first plays a central role in biology, and the second holds promise for analogous significance in nanotechnology applications. While each structure in its natural form and environment is well established (e.g., the B-DNA form in solution,[1] or isolated CNTs[2]), their interaction has been the subject of intense investigation lately.[3−13] Segments of single-strand DNA are extremely flexible, strongly hydrophilic biopolymers, while CNTs are extremely stiff, strongly hydrophobic nanorods. This motivated many studies and possible applications. For example, CNTs are proposed to be used as the template for DNA encapsulation,[5] intracellular DNA transport,[6] DNA conformation transformation,[7] DNA hybridization,[8] electrochemical detection of DNA,[9] and ultrafast DNA sequencing.[10] A different set of applications involves single-stranded DNA (ssDNA) wrapping around CNTs in a diameter- and sequence-dependent manner, which would make it possible to dissolve the naturally hydrophobic CNTs in water and to sort them by their chirality.[3,4] Finally, ssDNA-decorated CNTs have been examined as a chemical sensor to discriminate gaseous odors,[11] while double-stranded DNA (dsDNA) in contact with a CNT array has been proposed as the basis for electronic switches involving electron transport in both components[12] and for high a k dielectrics field effect transistor.[13] Recent success in detecting DNA conformational changes[7] and hybridization[8] by near-infrared fluorescence of CNTs or CNT−field effect transistors[10] has opened the possibility of DNA sequencing through electronic means. What is currently missing from all of these attempts is a detailed understanding of the nature of the DNA−CNT interaction and its dependence on the nucleoside identity.

Here we investigate the interaction of individual DNA nucleosides with a CNT in vacuum and in the presence of external gate voltage. We propose a scheme to discriminate between nucleosides on CNTs based on measurement of electronic features through a local probe such as scanning tunneling spectroscopy (STS). We employed force field and ab initio quantum mechanical calculations to determine the detailed geometrical, energetic, and electronic features of single DNA nucleosides adsorbed on single-wall CNTs. The interaction between the nucleosides and the nanotube are described by van der Waals (vdW) forces and by forces due to their mutual polarization when they are in close contact. This interaction leads to distinct features in the electronic structure of the combined system, which are sufficiently dependent on nucleoside identity to allow for accurate identification, when the signal is processed by a carefully trained artificial neural network.

The basic idea for an experimental set up that will allow nucleoside identification is illustrated in Figure 1A: a fragment of ssDNA is brought in close contact with the CNT and wraps partially around it. A force can be exerted on one end of the DNA, for example, by attaching to a bead that can be manipulated by optical[14] or magnetic means.[15] This will lead to a situation in which a few (even a single) base is in intimate contact with the CNT. By pulling the ssDNA

* Corresponding author. E-mail: kaxiras@physics.harvard.edu.
[†] Department of Physics and Division of Engineering and Applied Sciences, Harvard University.
[‡] Department of Chemistry and Chemical Biology, Harvard University.
[§] Department of Biological Applications and Technology, University of Ioannina.

10.1021/nl0619103 CCC: $37.00
Published on Web 12/08/2006

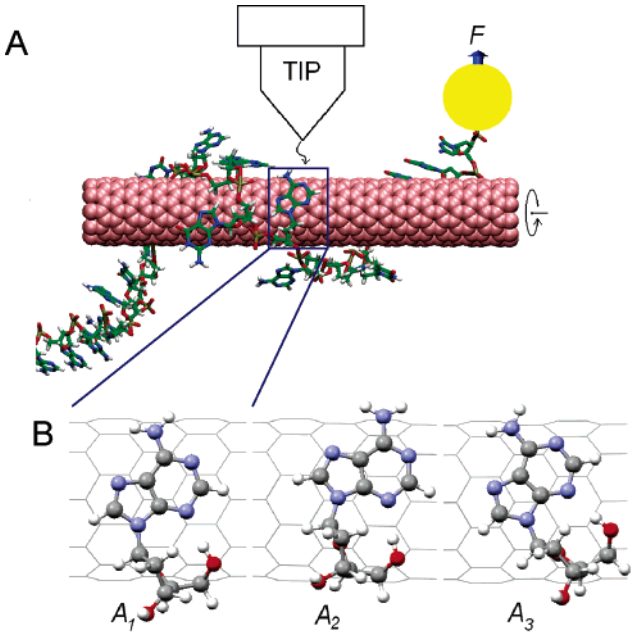

Figure 1. (A) Proposed experimental setup for single base measurement: a ssDNA fragment is in partial contact with the CNT and is being pulled at one end. (B) Representative optimal structures of adenine on the (10,0) CNT. The gray, blue, red, and white balls represent C, N, O, and H atoms, respectively.

fragment, the bases along it will successively interact with the CNT, allowing for measurements of the interaction. A setup in which the CNT can rotate in synchronization with the DNA pulling process may facilitate the motion. As a possible way of identifying the bases, we propose measuring the electronic structure of the combined system by a probe sensitive to local electronic states, such as STS, using a stationary scanning tunneling microscopy (STM) tip in the geometry similar to that in ref 16. This type of method has high resolution of ~2 Å and is routinely applied to investigate the local electronic structure of adsorbates on semiconductor surfaces.[17] To maximize the sensitivity of such measurements, it is desirable to have a semiconducting CNT as the substrate. Such a setup also overcomes the difficulty in the older proposals to distinguish DNA bases by measuring the transverse conductance of an electrode/ssDNA/electrode junction, where it is found that transverse conductance cannot be used to distinguish nucleotides because ssDNA is free and too flexible while in proximity to the electrode.[18] In our case here, the DNA is bound on the CNT, forming a very stable and robust complex that would constrain the DNA/electrode geometry in a desired, very well-controlled manner. The problem then involves identifying the relevant atomic geometries for a DNA nucleoside in contact with a semiconducting CNT and identifying the electronic signature of those combined structures, as it would be measured by an STS experiment. We address these two aspects of the problem separately.

To study the local interaction of DNA and CNTs microscopically, we used the nucleosides, consisting of a base, a deoxyribose sugar, and terminated by OH at the 3′ and 5′ ends. We focused our study on the semiconducting (10,0) nanotube; this nanotube, with a diameter of 7.9 Å, is abundant in CNT synthesis. Compared to the planar structure of graphite, CNTs have a curved structure that perturbs only slightly the nucleoside adsorption positions but results in many inequivalent adsorption geometries. We determined the energetically favorable configurations of the bases on the nanotube with the CHARMM program;[19] we augmented the CHARMM force field for nucleosides[20] with a force field for the CNT.[12] The CNT has a length along its axis equal to five times its repeat unit *c*. We performed the quantum mechanical calculations in the local density approximation (LDA) of the density functional theory (DFT) with the VASP code.[21] From these calculations, we obtained the electronic structure features that allowed us to determine the CNT−base signature.[22]

We performed an extensive search of the potential energy surface of each adsorbed nucleoside with the successive confinement method.[23] The potential energy surfaces of biomolecules are extremely complicated[24] and currently preclude direct exploration with ab initio methods. The search returned ~1000 distinct potential energy minima for each base−CNT system. This systematic search removed artificial bias about the possible geometries of the interacting system. The room-temperature populations of each minimum ranged from 10^{-10} to ~ 50%. Despite the numerous configurations, we found that only very few of them are dominant with significant room-temperature populations. For instance, there are three most stable configurations for A with populations 28.4%, 27.6%, and 10.1% (shown in Figure 1B). Together, these three structures represent ~65% of the total population of configurations. The remaining 35% of the population contains 808 configurations. Therefore, it is reasonable to focus on the dominant configurations only in our evaluation of the DNA−CNT interactions. Similarly, there are three most stable configurations for G, with populations of 45.9%, 20.8%, and 7.2%, four for C (populations: 25.2%, 6.8%, 4.3%, and 3.2%) and four for T (populations: 11.2%, 5.0%, 4.1%, and 2.0%). All of these configurations were included in our analysis of electronic features.

The preferred configurations for each base have certain similarities, but all are different from their ideal geometries upon adsorption on a planar graphene layer. The nucleoside binds on carbon nanotubes through its base unit, located 3.3 Å away from the CNT's wall. While the base unit remains planar without significant bending, the sugar residue is more flexible. It lies farther away from the CNT, usually having its OC_4 plane perpendicular to the CNT wall with the O atom pointing toward it (Figure 1B). On a graphene layer, the N and C atoms of A are found to occupy the hollow sites of the hexagonal rings.[25] Here, however, because of the curvature of the CNT, the C and N atoms of the base do not necessarily reside on the top of hexagonal C rings; instead they can shift position to maximize the vdW attraction between C, N, and O atoms in the base and C atoms in the CNT. Moreover, because the CNT structure is highly asymmetric with a long axis, the orientation of a base with respect to the tube axis can be very different. For instance, in one of the preferred geometries, C is rotated by 90° relative to the most stable configuration on graphene. Interestingly,

most of the dominant configurations upon nucleoside adsorption on the CNT are those with the sugar−base direction pointing perpendicular to the tube axis or slightly tilted. This geometry, consistent with previous simulations of ssDNA wrapped around CNTs,[4] would favor the binding of ssDNA on the CNTs, making nanotube dissolution and sorting more likely.

The force field approach discussed so far relies on empirically derived vdW interactions. In the context of the DFT/LDA quantum approach, it is the explicit polarization of electronic charge that contributes to interaction between the nucleosides and the CNT. The structures obtained from the force field calculations were further optimized using DFT/LDA until the calculated forces on each atom had a magnitude smaller than 0.005 eV/Å (which is considered a fully relaxed structure). The local structure, i.e., covalent bond lengths and bond angles, show minor changes (on the order of 0.02 Å and 1°), while the CNT−base distance was reduced by ∼0.3 Å. The base adsorption induced a very small distortion of the CNT geometry, consisting of a 0.02 Å indention of the side wall on the adsorption side and a 0.007 Å protrusion on the opposite side. The calculated interaction energy is 0.43−0.46 eV for A, C, G, and T in increasing order. This value is very close to the LDA calculation of adenine on graphite (0.46 eV),[25] but is significantly lower than the vdW energy of 0.7−0.8 eV from the CHARMM calculations. For comparison, the experimental value extracted from thermal desorption spectroscopy for A on graphite is 1.01 eV.[26]

The interaction between nucleosides and CNT, as described by the quantum approach, is illustrated in Figure 2A, where the isodensity surface of the charge density difference upon adsorption of A on CNT is shown. The interaction mainly involves the π orbitals of the base atoms, especially the NH_2 group at its end, and of the C atoms in the CNT. The mutual polarization of π orbitals in the DNA base and the CNT is more obvious in the planar-averaged charge density along the normal of the base plane, shown in Figure 2B. Upon adsorption, the base plane is positively charged, with electron accumulation (near the base) and depletion (near the CNT) in the region between the two components. Integrating this one-dimensional charge distribution in the base and the CNT region, respectively, reveals a net charge transfer of 0.017 *e* from A to the CNT. A detailed analysis of the contributions to the total energy of the system reveals that the attraction between the nucleoside and the CNT is due to exchange−correlation interactions, in agreement with similar calculations for A adsorbed on graphite[25] and on Cu surfaces.[27]

In electric measurements of the DNA−CNT system, a gate voltage is usually applied to control the conductance,[10] while the STM tip itself introduces a field on the order of 0.1 V/Å. Thermal fluctuations of counterions and water will average out to a zero contribution to the local field around the DNA−CNT system. We studied the effect of electric fields on DNA nucleoside adsorption on the CNT by treating the field as a planar dipole layer in the middle of vacuum region. The external field affects the interaction energy significantly

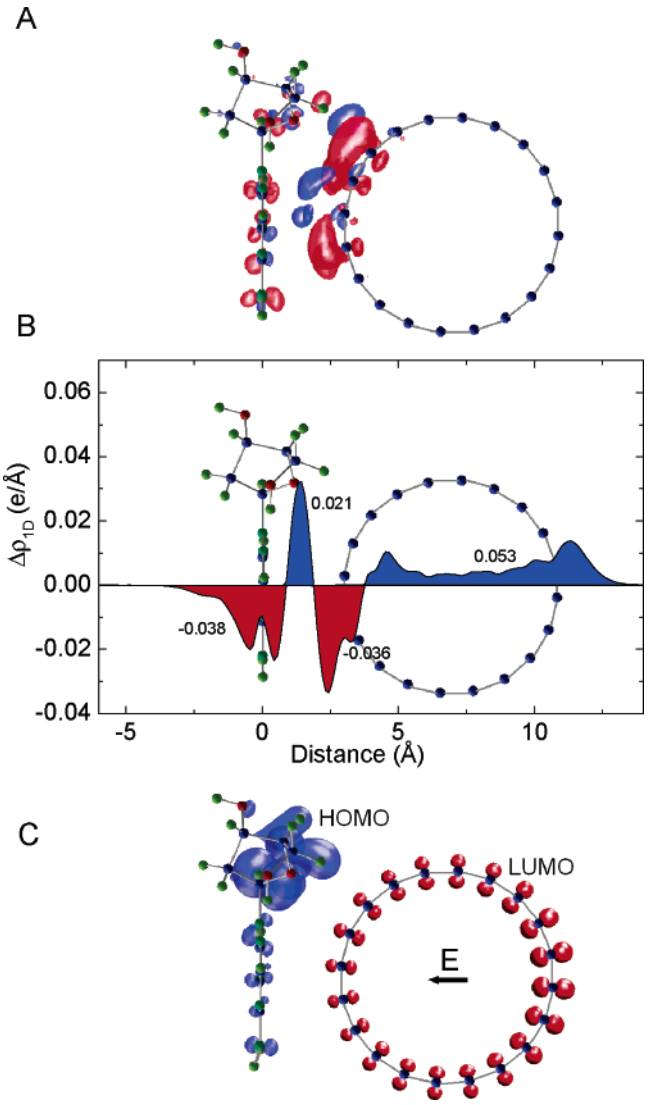

Figure 2. (A) Isodensity surface of the charge density differenceat levels of ±0.002 e/Å^3 in superposition to its atomic structure for A−CNT. The charge density difference is calculated by subtracting the charge density of the individual A and CNT systems, each fixed at their respective positions when they are part of the A−CNT complex, from the total charge density of the A−CNT combined system, i.e., $\Delta\rho = \rho$[A/CNT] − ρ[A] − ρ[CNT], where ρ is the charge density. Electron accumulation−depletion regions are shown in blue(+)/red(-). (B) One-dimensional charge density distribution, illustrating the mutual polarization of π orbitals. (C) The isodensity plot of HOMO and LUMO of A on CNT under an electric field of 0.5 V/Å.

(depending on the polarity), while it leaves almost unchanged the adsorption structure. Taking A−CNT as an example, we find that, although a negative field $E_{ext} = -0.5$ V/Å (CNT negatively charged) hardly changes the adsorption energy (0.436 eV), this energy increases significantly to 0.621, 0.928, and 1.817 eV under $E_{ext} = +0.25$, +0.5, and +1.0 V/Å, respectively. Here the adsorption energy in E_{ext} is defined as the energy difference between the total system under E_{ext} with respect to the energy of the CNT under E_{ext} and the free nucleoside. The base−CNT distance, on the other hand, only changes slightly: it is 0.04 Å larger than the zero field value for $E_{ext} = -0.5$ V/Å and 0.04 Å smaller for $E_{ext} = +1.0$ V/Å, respectively. The most prominent

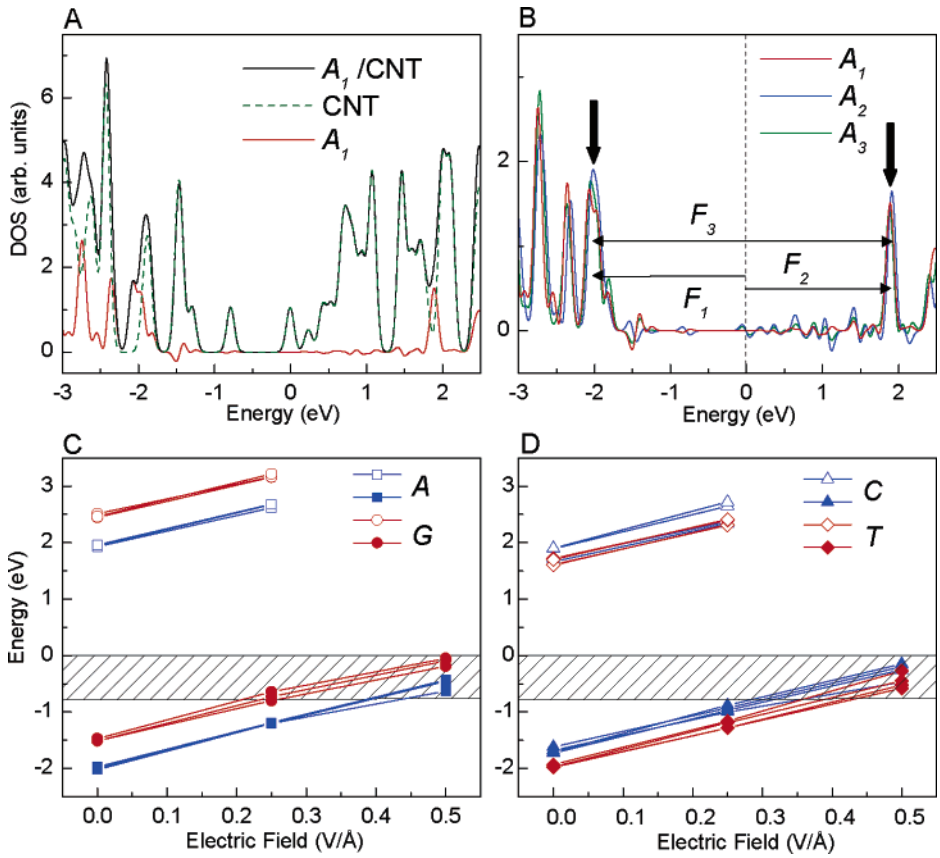

Figure 3. (A) DOS for adenine on the nanotube (A_1−CNT, solid black line), the CNT (dashed green line), and the difference ΔDOS (red line). The zero of the energy scale is set to the conduction band minimum of the CNT (same for the combined A_1−CNT system). (B) ΔDOS for three configurations of adenine on the CNT, labeled A_1, A_2, and A_3. The features F_1, F_2, and F_3 are identified. The HOMO and LUMO levels are indicated by vertical arrows. (C) Variation of the HOMO energy level (filled symbols) and the LUMO energy level (empty symbols) of A and G nucleosides on CNT. Shaded area is the energy gap of the CNT. (D) Same for the C and T nucleosides.

change in structure comes from the angle the NH_2 group at the end of the base makes with the base plane (Figure 2C). It switches from −27° at $E_{ext} = -0.5$ V/Å to +25° at $E_{ext} = +1.0$ V/Å, indicating the softness of C−NH_2 bond. The configuration under positive field resembles that on Cu(110).[27] Other nucleosides have the same behavior given their similarity in structure. Therefore, the applied electric field stabilizes the DNA bases on the CNT without disturbing the zero-field adsorption geometry. The more profound effect of the electric field lies in the change of electronic structure, discussed below.

The electronic density of states (DOS) describes the characteristic features of the electronic structure of a single DNA nucleoside adsorbed on the (10,0) CNT. The DOS peaks for the combined nucleoside−CNT system, Figure 3A, differ significantly from those of the bare CNT. The calculated energy gap of the CNT is 0.8 eV.[28] The difference in DOS between the bare CNT and one with a nucleoside (ΔDOS, red curve in Figure 3A for A) has features that extend through the entire range of energies; those close to the Fermi level are the most relevant for our discussion. These features can serve as the signal to identify DNA bases in current−voltage measurements (STS) or photoelectron spectroscopy. This "electronic fingerprint" is independent of the relative orientation of the nucleoside and the CNT, as shown in Figure 3B: the ΔDOS for the three dominant configurations of A on CNT have essentially the same features. The ΔDOS peaks for the different bases differ significantly from each other, which is encouraging as far as base identification is concerned. In parts C and D of Figure 3, we show the positions of the first peak below and above Fermi energy in the ΔDOS plots for A, C, G, and T adsorbed on the CNT. These two peaks correspond to the highest occupied molecular orbital (HOMO) and the lowest unoccupied molecular orbital (LUMO) of the bases, respectively. The HOMO and LUMO positions of the different bases are clearly distinguishable, while for a given base, the different adsorption geometries produce essentially indistinguishable peaks.

When a gate voltage is applied, the HOMO and LUMO peaks of the bases continuously shift with respect to the CNT DOS features. The latter change little under small gate voltage or an electric field. For example, the band gap of the CNT shrinks by only 0.03 eV for a field of $E_{ext} = 0.5$ V/Å, relative to its zero-field value. As is evident from Figure 3C,D, it is possible to induce a shift of the DNA base peaks relative to the CNT features with external voltage so as to facilitate experimental measurements. The HOMO and LUMO peaks of all bases shift monotonically with applied external field by ∼0.7 eV for $E_{ext} = 0.25$ V/Å. Interestingly, when the external field is sufficiently large, the HOMO of all four bases falls within the band gap of the CNT (see

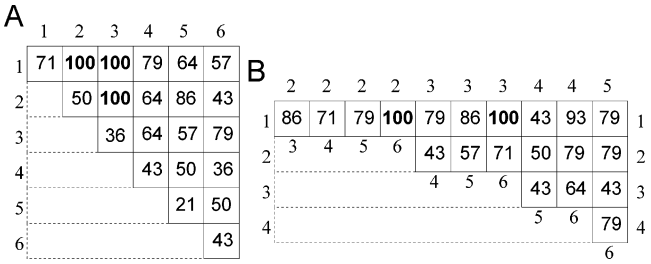

Figure 4. Efficiency (%) of DOS features in identifying DNA bases. (A) Efficiency of individual features and pairs of features at zero external field; the pairs F_1-F_2, F_1-F_3, and F_2-F_3 give perfect efficiency. (B) Efficiency of features taken in groups of three, at an external field of 0.25 eV/Å: the row number is the first feature, and the number at the top (bottom) of each column is the second (third) feature; the combinations $F_1-F_2-F_6$ and $F_1-F_3-F_6$ give perfect efficiency.

Figures 2C and 3C), which should enhance the sensitivity experimental measurements to the type of base. At the highest field we studied, $E_{ext} = 0.5$ V/Å, the band gap of the combined CNT−DNA systems is 0.51 eV for A, 0.45 eV for T, 0.27 eV for C, and 0.11 eV for G on average, sufficiently different from each other to be clearly distinguished.

To test the validity of the proposed detection of DNA bases through CNT−base interactions, we evaluated the efficiency of base identification using data generated from the ΔDOS calculations as input to a classifier, which was trained to produce as output the label of the DNA base (A, C, G, or T). Specifically, we extracted six simple representative features (F_i, $i = 1-6$) in an energy window from −3 to 3 eV around the Fermi level: (1) the location of the base HOMO, (2) the location of the base LUMO, (3) the band gap of the base (LUMO−HOMO distance), (4) the number of prominent peaks below the Fermi level, (5) the location of the highest occupied peak, and (6) the integral of the occupied states from −3 to 0 eV

The features F_1, F_2, and F_3 are indicated in Figure 3B for A. We produced a robust scheme for identifying the bases by employing artificial neural networks[29] and find that the network can deliver 100% efficiency, even after taking into consideration the measurement errors (e.g., an error of ± 0.10 eV in energy)[30] (see Figure 4). For practical applications, it is important to evaluate the significance of each feature individually. To this end, we tested the discriminating ability of each one of the six features defined and found that the location of base HOMO/LUMO (F_1/F_2) and the HOMO−LUMO gap (F_3) are the most informative features, while the number of occupied states (F_4) and the location of the highest peak (F_5) less so. The HOMO−LUMO gaps alone, which are 3.93−4.02 eV for A, 3.34−3.62 eV for C, 3.93−4.02 eV for G, and 3.58−3.69 eV for T, could easily discriminate A and G from C and T. Certain features are complementary, and combinations of just two features can actually yield 100% efficiency. For instance, if the location of HOMO (−2.02 eV for A, −1.68 eV for C, −1.51 eV for G, and −1.98 eV for T), which is well defined in experiments with respect to the DOS peaks of the CNT, is used in addition to the HOMO−LUMO gap, A is easily discriminated from G (and C from T), resulting in a 100% efficiency for the combination of features F_1-F_3. The external field magnifies these differences, making the base classification even more robust. With a field of 0.25 eV/Å, several triplets of features produce 100% efficiency in base identification (see Figure 4).

Acknowledgment. We thank Sergei Krivov for providing his implementation of the successive confinement approach. We acknowledge helpful discussions with J. Golovchenko and D. Branton.

References

(1) Watson, J. D.; Crick, F. H. C. *Nature (London)* **1953**, *171*, 737.
(2) Iijima, S. *Nature (London)* **1991**, *354*, 56.
(3) Zheng, M.; Jagota, A.; Strano, M. S.; Santos, A. P.; Barone, P.; Chou, S. G.; Diner, B. A.; Dresselhaus, M. S.; McLean, R. S.; Onoa, G. B.; Samsonidze, G. G.; Semke, E. D.; Usrey, M.; Walls, D. J. *Science* **2003**, *302*, 1545.
(4) Zheng, M.; Jagota, A.; Semke, E. D.; Diner, B. A.; McLean, R. S.; Lustig, S. R.; Richardson, R. E.; Tassi, N. G. *Nat. Mater.* **2003**, *2*, 338.
(5) Gao, H.; Kong, Y. *Annu. Rev. Mater. Res.* **2004**, *34*, 123.
(6) Kam, N. W. S.; Liu, Z.; Dai, H. *Angew. Chem., Int. Ed.* **2005**, *45*, 577.
(7) Heller, D. A.; Jeng, E. S.; Yeung, T.-K.; Martinez, B. M.; Moll, A. E.; Gastala, J. B.; Strano, M. S. *Science* **2006**, *311*, 508.
(8) Jeng, E. S.; Moll, A. E.; Roy, A. C.; Gastala, J. B.; Strano, M. S. *Nano Lett.* **2006**, *6*, 371.
(9) Li, J.; Ng, H. T.; Cassell, A.; Fan, W.; Chen, H.; Ye, Q.; Koehne, J.; Han, J.; Meyyappan, M. *Nano Lett.* **2003**, *3*, 597.
(10) Star, A.; Tu. E.; Niemann, J.; Gabriel, J.-C. P.; Joiner, C. S.; Valcke, C. *Prod. Natl. Acad. Sci. U.S.A.* **2006**, *103*, 921.
(11) Staii, C.; Johnson, A. T.; Chen, M.; Gelperin, A. *Nano Lett.* **2005**, *5*, 1774.
(12) Lu, G.; Maragakis, P.; Kaxiras, E. *Nano Lett.* **2005**, *5*, 897.
(13) Lu, Y.; Bangsaruntip, S.; Wang, X.; Zhang, L.; Nishi, Y.; Dai, H. *J. Am. Chem. Soc.* **2006**, *128*, 3518.
(14) Chu, S. *Science* **1991**, *253*, 5022.
(15) Smith, S. B.; Finzi, L.; Bustamante, C. *Science* **1992**, *258*, 1122.
(16) Kong, J.; LeRoy, B. J.; Lemay, S. G.; Dekker, C. *Appl. Phys. Lett.* **2005**, *86*, 112106.
(17) For example, local density of states of aniline ($C_6H_5NH_2$) on Si-(100) were clearly measured. Rummel, R.-M.; Ziegler, C. *Surf. Sci.* **1998**, *418*, 303.
(18) Zhan, X. G.; Krstic, P. S.; Zikic, R.; Wells, J. C.; Fuentes-Cabrera, M. *Biophys. J.* **2006**, *91*, L04.
(19) Brooks, B. R.; Bruccoleri, R. E.; Olafson, B. D.; States, D. J.; Swaminathan, S.; Karplus, M. *J. Comput. Chem.* **1983**, *4*, 187−217.
(20) MacKerell, A. D., Jr.; Bashford, D.; Bellott, R. L.; Dunbrack, R. L., Jr.; Evanseck, J. D.; Field, M. J.; Fischer, S.; Gao J.; Guo, H.; Ha, S.; Joseph-McCarthy, D.; Kuchnir, L.; Kuczera, K.; Lau, F. T. K.; Mattos, C.; Michnick, S.; Ngo, T.; Nguyen, D. T.; Prodhom, B.; Reiher, W. E., III; Roux, B.; Schlenkrich, M.; Smith, J. C.; Stote, R.; Straub, J.; Watanabe, M.; Wiorkiewicz-Kuczera, J.; Yin, D.; Karplus, M. *J. Phys. Chem. B* **1998**, *102*, 3586−3616.
(21) Kresse, G.; Hafner, J. *Phys. Rev. B* **1993**, *47*, 558.
(22) For these calculations, we employed a periodic supercell with dimensions of 20 Å × 20 Å × 3*c*. Larger supercells show minor differences in the structural and electronic features. A sampling of a 1 × 1 × 3 *k*-point mesh in reciprocal space is used to generate the charge density and the density of states. Gaussian smearing of electronic eigenvalues with a width of 0.1 eV is employed.
(23) Krivov, S. V.; Chekmarev, S. F.; Karplus, M. *Phys. Rev. Lett.* **2002**, *88*, 038101.
(24) (a) Elber, R.; Karplus, M. *Science* **1987**, *235*, 318. (b) Wales, D. J.; Scheraga, H. A. *Science* **1999**, *285*, 1368. (c) Wales, D. J. *Science* **2001**, *293*, 2067−2070.
(25) Ortmann, F.; Schmidt, W. G.; Bechstedt, F. *Phys. Rev. Lett.* **2005**, *95*, 186101.
(26) Freund, J. E. Ph.D. Thesis, Ludwig-Maximilians Universität, München, 1998.
(27) Preuss, M.; Schmidt, W. G.; Bechstedt, F. *Phys. Rev. Lett.* **2005** *94*, 236102.

(28) Ebbsen, T. W. *Carbon Nanotubes: Preparation and Properties*; CRC Press: Boca Raton, FL, 1997.
(29) Rumelhart, D. E.; Hinton, G. E.; Williams, R. J. *Nature* **1986**, *323*, 533−536.
(30) We used a standard feed-forward artificial neural network, the multilayer perceptron trained with the back-propagation algorithm and the leave-one-out cross-validation scheme implemented with the WEKA toolkit. Witten, I. H.; Frank, E. *Data Mining: Practical Machine Learning Tools and Techniques*, 2nd ed.; Morgan Kaufmann, San Francisco, 2005.

NL0619103